Critical minimum temperature limits xylogenesis and maintains treelines on the southeastern Tibetan Plateau

Citation

Published Version

Permanent link

Terms of Use

Share Your Story

Accessibility

Critical minimum temperature limits xylogenesis and maintains treelines on the southeastern Tibetan Plateau

Xiaoxia Li · Eryuan Liang · Jozica Gričar · Sergio Rossi · Katarina Čufar · Aaron M. Ellison

X. Li · E. Liang

Key Laboratory of Alpine Ecology and Biodiversity, Key Laboratory of Tibetan Environment Changes and Land Surface Processes, Institute of Tibetan Plateau Research, Chinese Academy of Sciences, Beijing 100085, China

E. Liang

CAS Center for Excellence in Tibetan Plateau Earth Sciences, Beijing 100101, China

J. Gričar

Slovenian Forestry Institute, Department of Yield and Silviculture, Vecna pot 2, SI-1000 Ljubljana, Slovenia

S. Rossi

University of Quebec in Chicoutimi, Département des Sciences Fondamentales, 555, Boulevard de l'Université, Chicoutimi (QC) G7H2B1, Canada ;

Key Laboratory of Vegetation Restoration and Management of Degraded Ecosystems, Guangdong Provincial Key Laboratory of Applied Botany, South China Botanical Garden, Chinese Academy of Sciences, Guangzhou 510650, China

K. Čufar

University of Ljubljana, Biotechnical Faculty, Department of Wood Science and Technology, Jamnikarjeva 101, SI-1000 Ljubljana, Slovenia

A. M. Ellison

Harvard Forest, Harvard University, 324 North Main St., Petersham, Massachusetts 01366, USA

Corresponding author (email: liangey@itpcas.ac.cn)

29   **Abstract**

30   Physiological and ecological mechanisms that define treelines are still debated. It has been suggested

31   that the absence of trees above the treeline is caused by low temperatures that limit growth. Thus, we

32   hypothesized that there is a critical minimum temperature (CT_{min}) preventing xylogenesis at treeline.

33   We tested this hypothesis by examining weekly xylogenesis across three and four growing seasons in

34   two natural Smith fir (*Abies georgei* var. *smithii*) treeline sites on the southeastern Tibetan Plateau.

35   Despite differences in the timing of cell differentiation among years, minimum air temperature was

36   the dominant climatic variable associated with xylem growth; the critical minimum temperature

37   (CT_{min}) for the onset and end of xylogenesis occurred at 0.7±0.4 °C. A process-based modelling

38   chronology of tree-ring formation using this CT_{min} was consistent with actual tree-ring data. This

39   extremely low CT_{min} permits Smith fir growing at treeline to complete annual xylem production and

40   maturation and provides both support and a mechanism for treeline formation.

41

42   **Keywords:** Cambial activity • critical minimum temperature • timberline • xylem • Vaganov-Shashkin

43   model

44

1 Introduction

The explanations for treeline formation focus on limitations of available resources [1, 2],

establishment sites [3], or time available for growth [4], although these ecophysiological causes

remain debated [5-8]. Based on notable similarities in temperatures at treelines [9], the growth

limitation hypothesis proposed that low temperatures limit the time available for meristematic growth

and cell division [4, 10]. This hypothesis has been supported by phenomenological data. For example,

treeline trees tend to have higher amounts of non-structural carbohydrates than trees growing at lower

elevation, suggesting that treeline is limited more by growth processes than by photosynthesis and

carbon assimilation [11-13]. In parallel, dendroclimatic studies have identified a signal of reduced

growth during periods with low temperatures at treelines in cold and humid areas [14-17].

Physiological manifestations of the growth limitation hypothesis include a constraint on the

production of new cells by meristems below a critical minimum temperature (CT_{min}) [4] and a

trade-off between taking maximal advantage of the length of the growing season while avoiding

cellular damage due to early (fall, winter) or late (winter, spring) freezing events [18-19]. Such a

trade-off would suggest a narrow thermal window for the onset and cessation of xylogenesis at

treeline and recent studies have described temporal dynamics in xylogenesis of various tree species at

treeline [20-24]. Some studies reported that a gradual increase in temperature (heat sum) was

associated with the onset of cambial activity [21, 25], whereas others estimated a CT_{min} of 6 - 8 °C for

xylogenesis at the altitudinal treeline in the Eastern Alps [20, 26]. Separating gradual (heat-sum) and

threshold (CT_{min}) effects on xylogenesis at treeline has not yet been accomplished.

A mechanistic model can provide a deeper understanding on the climatic control on tree growth

dynamics. The process-based Vaganov-Shashkin (VS) model has been used to simulate climatic

controls on conifer tree-ring growth [27-29]. In the VS model, the critical temperature for cambial

activity is a key parameter for modelling tree growth, but there are limited data available to estimate

this parameter.

Our observations at the upper treeline of Smith fir (*Abies georgei* var. *smithii*) on the southeastern

Tibetan Plateau, including a decade of uninterrupted *in situ* micrometeorological measurements and

weekly collection of microcores containing cambium activity and wood formation during three

consecutive growing seasons provide an opportunity to examine both gradual and threshold effects of

temperature on xylogenesis at a natural alpine treeline. Specifically, we tested the potential for

75 thermal control of xylogenesis to be a mechanism underlying the growth limitation hypothesis by (1)

76 identifying the timing and dynamics of xylogenesis in Smith fir growing at treeline as a function of

77 climatic factors; and (2) detecting a plausible CT_{min} for xylogenesis. Previous studies have found that

78 the growth of Smith fir near treeline is constrained by the minimum temperature in summer [30, 31].

79 The onset of bud swelling and needle unfolding in Smith fir is delayed by 3.5 days for each 100-m

80 increase in elevation [32], indicating a thermal limitation of tree phenology. Therefore, we

81 hypothesized that minimum temperature limits xylogenesis and that a threshold minimum temperature

82 controls the timing of the onset and ending of xylogenesis.

83

84 **2 Materials and methods**

85 **2.1. Study sites and tree selection**

86 We studied the natural alpine treeline of Smith fir growing on the eastern side of the Sygera

87 Mountains (29° 10′ – 30° 15′ N, 93° 12′ – 95° 35′ E) on the southeastern Tibetan Plateau [33]. The

88 southeastern Tibetan Plateau is characterized by a cold and humid climate, and has the highest natural

89 treeline (up to 4900 m a.s.l.) in the Northern Hemisphere [34]. Smith fir is a shade tolerant tree

90 species and is one of the dominant treeline species in this region. The upper treeline position depends

91 on topographic aspect and ranges from 4250 to 4400 m a.s.l. We studied two sites at open-canopy

92 treelines: site 1 was at 4360 m a.s.l. on an east-facing slope, and site 2 was at 4250 m a.s.l. on a

93 southeast-facing slope. The sites were 200 m apart, on slopes < 15°. *Rhododendron aganniphum* var.

94 *schizopeplum* dominated the understory. The coverage of Smith fir was < 20% and the podzolic soils

95 had an average pH value of 4.5.

96   At each site, five dominant trees were selected in April 2007. These trees had a mean age of 201

97 ± 24 and 117 ± 14 years, and mean diameters at 1.3 m aboveground of 34 ± 4 and 44 ± 7 cm in sites 1

98 and 2, respectively. Because repeated sampling could cause severe wounding that could modify

99 xylogenesis, another five trees per site with similar diameters at breast height were chosen for

100 samplings in 2009 and 2010. Trees with polycormic stems, partially dead crowns, reaction wood, or

101 other evident damage were avoided.

102

103 **2.2 Meteorological data**

104 An automatic weather station (Campbell Scientific, CR1000) was installed in November 2006 in an

4

105   open area above the treeline (29°39′ N, 94°42′E, 4390 m a.s.l.) at a linear distance of ≈150 m and 200

106   m from sites 1 and 2, respectively. Measurements of air (3 m aboveground) and soil temperature (at

107   10-, 20- and 40-cm depths), precipitation, snow fall, and soil water content (at 10-, 20-, and 40-cm

108   depths) were collected at 30-minute intervals. These data were used to compute daily averages,

109   minima, and maxima of each variable.

110

111   **2.3 Microcoring and histological analyses**

112   Xylem growth was studied from 2007 until 2010 at site 1 and from 2007 to 2009 at site 2. One

113   microcore (15-mm long, 2-mm diameter) was collected from each tree weekly from May until

114   October around the stem at breast height (1.3 m aboveground) using a Trephor tool. Immediately after

115   removal from the trees, the microcores were fixed in a formalin-ethanol-acetic acid (FAA) solution.

116   The microcores contained innermost phloem, cambium, developing xylem, and at least three previous

117   xylem growth rings. In the laboratory, the microcores were dehydrated with successive immersions in

118   a graded series of ethanol and d-limonene, then embedded in paraffin. Transverse sections (9–12 μm

119   in thickness) were cut from the samples with a Leica RM 2245 rotary microtome using Feather N35H

120   knives (Osaka, Japan). Sections were stained with a mixture of safranin (0.5 % in 95 % ethanol) and

121   astra blue (0.5 % in 95% ethanol) and observed with a Nikon Eclipse 800 light microscope under

122   bright field and polarized light to identify the phases of differentiation of the developing xylem cells

123   [35]. In cross-section, cambial cells were characterized by thin cell walls and small radial diameters

124   [36, 37]. Newly-formed xylem cells in the phase of cell enlargement contained protoplasts, had thin

125   primary walls, and a radial diameter at least twice the size of the cambial cells [38]. The onset of

126   cell-wall thickening was determined by birefringence in the cell walls under polarized light. Mature

127   cells had completely red-stained walls and empty lumen. For each sample, the total current xylem cell

128   number was determined by counting the number of cells undergoing enlargement, cell-wall thickening,

129   and the number of mature cells along three radial files.

130

131   **2.4 Data standardization and fitting of xylem growth**

132   The data were standardized to compensate for variation in the number of xylem cells along the tree

133   circumference. The total cell number of the previous years was counted on three radial files per

134   sample and used for standardization. The standardized number of cells nc_{ij} in the ith phase of the jth

135 sample was calculated as:

$$nc_{ij} = n_{ij} \, (a_m / a_j) \tag{1}$$

137 where n_{ij} is the number of cells in the current year, a_m is the mean number of cells of the previous ring

138 of all j-samples, and a_j is the mean number of cells of the previous ring in each j-sample .

139   We modelled the dynamics of xylem growth by fitting a Gompertz function to the number of

140 xylem cells that were produced through time:

$$y = A\exp[-\, e^{(\beta \, -\kappa t)}] \tag{2}$$

142 where y is the weekly cumulative sum of tracheids, t is the time of the year computed as day of the

143 year, A is an asymptote (constant), and β and k are constants reflecting the x-intercept placement and

144 rate of change, respectively. Model parameters were estimated using the Origin software package

145 (Version 8.5, OriginLab Corporation, Northampton, MA, USA).

146

147 **2.5 Estimation of the onset and ending of xylogenesis**

148 We used observations of cell differentiation to identify the onset, ending, and duration of xylogenesis

149 from counts of the number of cells in three radial files per tree. In spring, xylogenesis was considered

150 to have started when at least one tangential row of cells was observed in the enlarging phase. Because

151 of the weekly resolution of the monitoring, we used the occurrence of 1–2 enlarging xylem cells along

152 any of the checked three radial files as an indicator the xylogenesis had begun [35]. In late summer,

153 when cells were no longer observed in the wall thickening and lignification phase, xylogenesis was

154 considered to have ended. The duration of xylogenesis was estimated as the number of days between

155 the dates of onset and ending of xylogenesis.

156   Comparisons between sites in onset, duration, and ending of differentiation in the developing

157 xylem ring were done with generalized linear models (GLM). Homoscedasticity was checked using

158 Shapiro-Wilk and Levene tests.

159

160 **2.6 Identifying CT$_{min}$**

161   Logistic regression (LOGISTIC procedure in SPSS 16.0) was used to model the probability of

162 xylogenesis as a function of air temperature. Xylogenesis was coded as zero (not occurring) or one

163 (occurring). CT$_{min}$ was estimated as that temperature for which the probability of ongoing xylem

164 growth equalled 0.5 [39]. For each tree and year, the model was fitted with three respective daily

165   temperature series (mean, minimum, and maximum). Therefore, the CT_{min} represents the critical night

166   temperature for xylogenesis. Model verification included the likelihood-ratio χ^2, Wald's χ^2 for

167   regression parameter and goodness of fit, and Hosmer-Lemeshow $\hat{C}$ for possible lack of fit. None of

168   the models were excluded because of a lack of fit. CT_{min} values were compared between sites and

169   years using analysis of variance (ANOVA) models. Model validation was performed by comparing

170   the observed and predicted CT_{min} values. Degree-day sum (DD) is an index representing a measure of

171   accumulated heat. In spring, accumulation of DD began when daily air average temperature $\geq 5°C$ for

172   five consecutive days. The temperature $5°C$ is a commonly used standard in calculating the effective

173   heat sum in agriculture and forestry [40].

174

175   **2.7 Climate-growth relationships**

176   We used two approaches to identify relationships between intra-annual xylem growth and climatic

177   variables during four growing seasons. One approach consisted of computation of Pearson's

178   correlation coefficients between xylem cell production and weather data for weekly intervals. Weather

179   data here include daily mean, daily absolute minimum, daily absolute maximum temperatures,

180   growing degree-days (GDD) $> 5°C$, and sums of precipitation.

181   Intra-annual xylem growth may be controlled both by endogenous (e.g., hormonal regulation)

182   and exogenous factors (e.g., climate). To analyse the climatic effect, a common approach was used to

183   remove the endogenous growth trend by fitting a growth curve, and to estimate the growth departure,

184   calculated as the dimensionless ratio between observed and expected growth [41]. This ratio

185   (hereafter called the 'growth index') was calculated as the number of tracheids produced during the

186   week divided by the expected values estimated using the Gompertz function [42]. To account for

187   possible effects of time-lags, daily weather data were averaged (temperature) or summed

188   (precipitation) weekly from 1 to 10 d prior to each sampling date (referred to as P1 to P10). To

189   minimize the effects of temporal autocorrelation, correlation coefficients were calculated on

190   first-order differences for both datasets.

191

192   **2.8 Tree-ring modeling**

193   We used the Vaganov-Shashkin (VS) model to simulate tree-ring growth at the Smith fir treelines in

194 the Sygera Mountains. The VS model estimates xylem growth and its internal characteristics based on

195 equations relating daily temperature, precipitation, and sunlight to the kinetics of xylem development

196 [43]. It assumes that climatic influences are directly but nonlinearly related to tree-ring characteristics

197 through controls on the rates of cambial activity processes. To date, it has been successfully used to

198 simulate and evaluate the relationships between climate and tree-ring formation under a variety of

199 environmental conditions in many different regions [28, 29, 44-47]. Values from field observations

200 were used for input parameters needed by the VS model: soil moisture, depth of root system,

201 temperature sum for initiation of growth, soil water drainage rate, and maximum daily precipitation

202 infiltrating into soil. We used our estimates of CT_{min} as the starting value for the minimum

203 temperature parameter. Model fit was evaluated against an actual tree-ring width chronology from

204 Smith fir treeline in the Sygera Mts., which had been developed and used for paleoclimatic

205 reconstructions in this region [31]. The best estimate of physiological CT_{min} was found by iteration

206 and comparison between simulated and observed chronologies (1960 – 2006).

207   Finally, a single simulated tree-ring width chronology was created for the Smith fir treeline in the

208 Sygera Mts. based on daily climate data from the Nyingchi meteorological station (3,000 m a.s.l.). To

209 account for the altitude differences between Nyingchi and the study sites, we extended the time series

210 of daily temperatures at the treeline back to 1960 based on a linear regression of the Nyingchi data

211 and our own micrometeorological data ($r \geq 0.89$, 2007–2010, Supporting Information Fig. S1).

212

213 **3 Results**

214 **3.1 Micrometeorological conditions at the upper treeline**

215 The sampling sites at the upper treeline were cold and humid. Despite a difference of 110 m in

216 elevation and different topographical aspects of the two treeline sites, they had similar temperatures

217 (Supporting Information Fig. S2). Annual average temperatures (2007 – 2010) ranged from 0.1 to 0.9

218 °C, while growing-season (June-September) temperatures ranged from 6.4 to 7.1 °C (Fig. 1). On

219 average, annual precipitation was 951 mm, of which 62 % fell during the monsoon season (June to

220 September). Snowfall occurred mainly from November to May. Because of snowmelt and increased

221 precipitation, soil moisture content increased rapidly from the beginning of April and remained above

222 30% from early May until November, and finally decreased to near zero in late November and early

223 December. The year 2008 was characterized by heavy spring snowfall and had the latest snowmelt

224   and soil thawing during the four studied years (Fig. 1).

225

226   **3.2 Xylogenesis**

227   The onset of xylogenesis occurred from late May to early June and differed significantly among years

228   ($F = 15.73$, $P < 0.001$). The onset of xylogenesis was observed 4 – 9 days later in 2008 than in the

229   other years, at both sites (Fig. 2 a). No difference was found in onset of xylogenesis between sites (F

230    $= 2.31$, $P > 0.05$). Xylogenesis ended between the beginning and the end of September and differed

231   significantly among years ($F = 10.42$, $P < 0.005$), and occurred 1–2 weeks later in 2010 at site 1 (Fig.

232   2 b).

233   Overall, the duration of xylogenesis lasted from 109 to 125 days (Fig. 2 c), with no significant

234   differences detected between sites ($F = 3.80$, $P > 0.05$). Conversely, there were significant variations

235   among years ($F = 4.71$, $P < 0.05$). From 2007 to 2009, the average period between the onset and

236   ending of xylogenesis was 113 days, whereas the average of 125 days was required to complete

237   xylogenesis in 2010.

238

239   **3.3 Relationship between climate and xylem growth**

240   Weekly cumulative xylem production was fit well by the Gompertz function ($0.96 \leq r^2 \leq 0.98$;

241   Supporting Information Table S1 and Fig. S3). Intra-annual xylem cell production was significantly

242   and positively correlated with daily minimum and mean air temperatures and GDD > 5 °C at both

243   sites (Fig. 3 a, b). However, only minimum temperature was significantly correlated with growth

244   indices after removing the growth trends (Figs. 3 c, d). At site 1, positive correlations between growth

245   indices and minimum temperatures were found for time lags of 0 – 3 days ($r = 0.34$, $P < 0.05$),

246   whereas the corresponding time lags were 7 – 10 days at site 2 ($r = 0.42$, $P < 0.05$). No significant

247   correlations were found between xylem cell production or growth index and precipitation from P0 to

248   P10.

249

250   **3.4 CT_{min}**

251   The critical minimum air temperature (CT_{min}) at which there was a 0.5 probability that xylem

252   formation was ongoing is shown in Fig. 4 and Table 1 for site 1 (2007 – 2010) and site 2 (2007 –

253   2009). The values for minimum, mean, and maximum temperatures of 0.6, 4.0, and 9.3 °C were

254   estimated for the onset of xylogenesis, whereas the corresponding values for the ending of xylem

255   differentiation were 0.7, 3.9, and 9.0 °C. There were no differences among critical temperatures for

256   the onset and ending of xylogenesis (ANOVA, $P > 0.05$), with values of 0.7 ± 0.4, 3.9 ± 0.5, and $9.1 \pm$

257   0.6 °C for the minimum, mean, and maximum temperatures, respectively. No significant differences

258   were found between the two sites in terms of the estimated air temperature thresholds for the onset

259   and ending of xylogenesis (ANOVA, $P > 0.05$). The mean air temperature during the period of xylem

260   formation at both sites was 6.8 ± 0.4°C.

261   Among years, degree-day sum until the onset of xylogenesis at site 1 ranged from 8–41 DD,

262   whereas corresponding temperature sums ranged from 12–34DD at site 2 (Table 2). Accumulated heat

263   sum from 1 January until onset of xylem growth varied strongly between study years at both sites ($F=$

264   17.6, $P < 0.01$).

265

266   **3.5 Tree-ring modelling**

267   Initializing the Vaganov-Shashkin (VS) model with with an estimated $CT_{min} = 0.7$ °C yielded a best-fit

268   estimate of physiological $CT_{min} = 0.9$ °C (Table 3, Fig. 5). The correlation between observations and

269   predictions varied slightly for CT_{min} of 0.3–1.0 °C, whereas it decreased rapidly for $CT_{min} > 1$ °C (Fig.

270   6). Overall, significant, positive correlations were found between the modelled and measured

271   chronologies when CT_{min} varied within the range of 0.7 ± 0.4°C ($r = 0.62$, $P < 0.01$).

272

273   **4 Discussion**

274   The importance of temperature for xylogenesis during and after its onset has been demonstrated

275   repeatedly [25, 37, 48-51]. These and other data suggest that air temperature, not soil temperature,

276   directly limits xylogenesis at high latitudes and altitudes [20, 24, 52]. Minimum temperature is

277   assumed to be an important driver of tree species range limits [7, 19], and so a critical minimum

278   temperature (CT_{min}) with narrow bounds should exist for the onset and ending of xylogenesis.

279   However, long-term monitoring of xylem growth at natural treelines is limited, which has precluded

280   assessment of CT_{min} for xylogenesis by direct observations.

281

282   **4.1 Effects of climate on xylem growth**

283   As predicted, minimum air temperature strongly limited xylem growth of Smith fir at the upper

284   treeline on the southeastern Tibetan Plateau. This finding agrees with those from dendroclimatological

285   analysis in the same study area [31] and wood formation studies at high latitudes and altitudes [22,

286   37]. The importance of minimum air temperature may be related to the timing of cell differentiation,

287   which may occur mainly during the night when the temperature is lower [53, 54]. Controlled

288   experiments also showed that night temperatures could directly influence xylem cell expansion of

289   *Podocarpus latifolius* [55]. According to Körner [7], cell doubling time, which is highest and fairly

290   constant at temperatures of 10–25°C, approaches infinity at 1–2°C, suggesting a minimum

291   temperature limit on cell division. The simulated ring-width chronologies produced by the VS model

292   of tree-ring formation also exhibit similar positive correlations with the minimum temperature during

293   summer (Supporting Information Fig. S4, $P < 0.01$). CT_{min} is thus expected to limit xylogenesis of

294   Smith fir at the treeline.

295

296   **4.2 Critical temperatures for xylogenesis**

297   Our results suggest that threshold effects, not heat sum effects, play a key role in the onset of

298   xylogenesis at Smith fir treeline. Despite the variance in timing and duration of xylogenesis during

299   our four years of observations, minimum, average, and maximum temperatures for the onset and

300   ending of xylogenesis were narrowly bounded with average values of 0.7, 3.9, and 9.1 °C,

301   respectively.

302   Most studies to date have indicated that xylogenesis in conifers growing in cold climates can take

303   place when the daily minimum temperatures $\geq$ 4–5 °C [39, 56]. However, based on the presented

304   4-year observations of xylogenesis and uninterrupted *in situ* micrometeorological measurements

305   directly at the treeline, we found that the CT_{min} for xylogenesis in Smith fir is as low as 0.7 °C. In

306   particular, based on this CT_{min} , the modelled chronology produced by VS model is consistent with

307   actual tree-ring data, suggesting that minimum temperature could be considered as a significant driver

308   of xylem growth. Such a low CT_{min} may have evolved to provide sufficient time to complete

309   xylogenesis at alpine treelines. The length of the growing season for stem growth diminishes with

310   altitude and reaches a minimum at the alpine treeline. According to some authors [10, 39], a tree can

311   only survive when the growing seasons are at least 3 months long and the mean air temperature during

312   the growing season is 6.4.°C; each of these constraints critically limit the growth and development of

313   trees. At Smith fir treelines in southeastern Tibet, the duration of xylem growth of 115 days provided

314   by a $CT_{min} < 1\ °C$ and a mean air temperature of 6.8 °C during the growing season extended by this

315   low CT_{min} together meet these prerequisites for tree growth and development.

316   The dates of snow melting and soil thawing also are thought to be critical for the onset of

317   xylogenesis and could therefore determine the annual xylem production [27]. At our treeline sites, the

318   onset of xylem growth occurred 4-46 days after snow melting and 4-29 days after soil thawing in

319   spring, which coincided with the surpassing of CT_{min} (Table 2). This temporal lag also suggests that

320   threshold effects exist for the onset of xylogenesis at Smith treeline.

321   The growth limitation hypothesis predicts that the absence of trees above the treeline is

322   attributable to critical minimum temperature for growth [4]. Treeline trees often have slower growth

323   rates and higher non-structural carbohydrate levels than trees at lower altitudes [11-13], suggesting a

324   carbon sink rather than carbon gain limitation [57]. However, some authors have argued that tree

325   populations with the highest non-structural carbohydrate concentrations may be the most carbon

326   limited in terms of growth [58, 59]. Although our observations of xylogenesis cannot differentiate

327   between carbon limitation and a carbon sink in Smith fir, the significant effect of a narrowly bounded

328   CT_{min} on xylem growth provides a physiological mechanism for the growth limitation hypothesis.

329

338

339   **Conflict of interest**   The authors declare that they have no conflict of interest.

340

341   # References

342   1. Stevens GC, Fox JF (1991) The Causes of Treeline. Ann. Rev. Ecol. Sys. 22: 177-191.

343 2. Susiluoto S, Hilasvuori E, Berninger F (2010) Testing the growth limitation hypothesis for

344   subarctic Scots pine. J. Ecol. 98: 1186-1195.

345 3. Smith WK, Germino MJ, Hancock TE et al (2003) Another perspective on altitudinal limits of

346   alpine timberlines. Tree Physiol 23: 1101-1112.

347 4. Körner C (1998) A re-assessment of high elevation treeline positions and their explanation.

348   Oecologia 115: 445-459.

349 5. Tranquillini W (1979) Physiological ecology of the alpine timberline. Springer, Berlin Heidelberg

350   New York.

351 6. Holtmeier FK (2003) Mountain timberlines: ecology, patchiness and dynamics. Dordrecht, Kluwe.

352 7. Körner C (2003) Alpine plant life: functional plant ecology of high mountain ecosystems, 2nd edn.

353   Springer, Berlin Heidelberg New York.

354 8. Cui H, Liu H, Dai J (2005) Study on mountain ecology and alpine timberline. Beijing, Science

355   Press.

356 9. Körner C, Paulsen J (2004) A world-wide study of high altitude treeline temperatures. J. Biogeogr.

357   3: 713-732.

358 10. Körner C (2012) Alpine treelines: functional plant ecology of the global high elevation tree limits.

359   Springer, Berlin Heidelberg New York.

360 11. Hoch G, Körner C (2003) The carbon charging of pines at the climatic treeline: a global

361   comparison. Oecologia 135: 10-21.

362 12. Shi P, Körner C, Hoch G (2008) A test of the growth-limitation theory for alpine tree line

363   formation in evergreen and deciduous taxa of the eastern Himalayas. Funct Ecol 22: 213-220.

364 13. Fajardo A, Piper FI, Hoch G (2013) Similar variation in carbon storage between deciduous and

365   evergreen treeline species across elevational gradients. Ann Bot 112: 623-631.

366 14. Makinen H, Nojd P, Mielikainen K (2000) Climatic signal in annual growth variation of Norway

367   spruce (*Picea abies*) along a transect from central Finland to the Arctic timberline. Can J For Res

368   30: 769-777.

369 15. Oberhuber W (2004) Influence of climate on radial growth of *Pinus cembra* within the alpine

370   timberline ecotone. Tree Physiol 24: 291-301.

371 16. Frank D, Esper J (2005) Characterization and climate response patterns of a high-elevation,

372   multi-species tree-ring network in the European Alps. Dendrochronologia 22: 107-121.

373   17. Ettinger AK, Ford KR, HilleRisLambers J (2011) Climate determines upper, but not lower,
374   altitudinal range limits of Pacific Northwest conifers. Ecology 92: 1323-1331.

375   18. Chuine I, Beaubien EG (2001) Phenology is a major determinant of tree species range. Ecol Lett 4:
376   500-510.

377   19. Kollas C, Körner C, Randin CF (2014) Spring frost and growing season length co-control the cold
378   range limits of broad-leaved trees. J Biogeogr 41: 773-783.

379   20. Rossi S, Deslauriers A, Anfodillo T et al (2007) Evidence of threshold temperatures for
380   xylogenesis in conifers at high altitudes. Oecologia 152: 1-12.

381   21. Seo JW, Eckstein D, Jalkanen R et al (2008) Estimating the onset of cambial activity in Scots pine
382   in northern Finland by means of the heat-sum approach. Tree Physiol 28: 105-112.

383   22. Gruber A, Baumgartner D, Zimmermann J et al (2009) Temporal dynamic of wood formation in
384   *Pinus cembra* along the alpine treeline ecotone and the effect of climate variables. Trees- Struct
385   Funct 23: 623-635.

386   23. Moser L, Fonti P, Büntgen U et al (2010) Timing and duration of European larch growing season
387   along altitudinal gradients in the Swiss Alps. Tree Physiol 30: 225-233.

388   24. Lenz A, Hoch G, Körner C (2012) Early season temperature controls cambial activity and total
389   tree ring width at the alpine treeline. Plant Ecol Diver 6: 365-375.

390   25. Jyske T, Makinen H, Kalliokoski T et al (2014) Intra-annual tracheid production of Norway
391   spruce and Scots pine across a latitudinal gradient in Finland. Agric. For. Meteorol., 194:
392   241-254.

393   26. Ziaco E, Biondi F, Rossi S et al (2016) Environmental drivers of cambial phenology in Great
394   Basin bristlecone pine. Tree Physiol 36: 818-831.

395   27. Vaganov EA, Hughes MK, Kirdyanov AV et al (1999) Influence of snowfall and melt timing on
396   tree growth in subarctic Eurasia. Nature 400: 149-151.

397   28. Anchukaitis KJ, Evans MN, Kaplan A et al (2006) Forward modeling of regional scale tree-ring
398   patterns in the south-eastern United States and the recent influence of summer drought. Geophys
399   Res Lett 33: L04705.

400   29. Evans MN, Reichert BK, Kaplan A et al (2006) A forward modeling approach to paleoclimatic
401   interpretation of tree-ring data. J Geophys Res-Biogeo. 111: G03008.

402   30. Bräuning A, Mantwill B (2004) Summer temperature and summer monsoon history on the Tibetan

403   plateau during the last 400 years recorded by tree rings. Geophys Res Lett 31: L24205.

404   31. Liang E, Shao X, Xu Y (2009) Tree-ring evidence of recent abnormal warming on the southeast

405   Tibetan Plateau. Theor Appl Climatol 98: 9-18.

406   32. Wang Y, Li X, Dawadi B et al (2013) Phenological variation in height growth and needle

407   unfolding of Smith fir along an altitudinal gradient on the southeastern Tibetan Plateau. Trees -

408   Struct Funct 27: 401-407.

409   33. Liang E,Wang Y, Eckstein D et al (2011) Little change in the fir tree-line position on the

410   south-eastern Tibetan Plateau after 200 years of warming. New Phytol. 190: 760-769.

411   34. Miehe G, Miehe S, Vogel J et al (2007) Highest treeline in the northern hemisphere found in

412   southern Tibet. Mount Res Devel 27: 169-173.

413   35. Li X, Liang E, Gričar J et al (2013) Age dependence of xylogenesis and its climatic sensitivity in

414   Smith fir on the south-eastern Tibetan Plateau. Tree Physiol 33: 48-56.

415   36. Deslauriers A, Morin H, Begin Y (2003) Cellular phenology of annual ring formation of *Abies*

416   *balsamea* in the Quebec boreal forest (Canada). Can J Forest Res 33: 190-200.

417   37. Camarero JJ, Olano JM, Parras A (2010) Plastic bimodal xylogenesis in conifers from continental

418   Mediterranean climates. New Phytol 185: 471-480.

419   38. Rathgeber CBK, Rossi S, Bontemps JD (2011) Cambial activity related to tree size in a mature

420   silver-fir plantation. Ann Bot 108: 429-438.

421   39. Rossi S, Deslauriers A, Gričar J et al (2008) Critical temperatures for xylogenesis in conifers of

422   cold climates. Global Ecol Biogeogr 17: 696-707.

423   40. Monteith JL (1981) Climate variation and the growth of crops. Q J R Meteorolog Soc 107:

424   749-774.

425   41. Fritts H (1976) Tree rings and climate. Academic Press, New York.

426   42. Zhai L, Bergeron Y, Huang J et al (2012) Variation in intra-annual wood formation, and foliage

427   and shoot development of three major Canadian boreal tree species. Am J Bot 99: 827-837.

428   43. Vaganov EA, Hughes MK, Shashkin AV (2006) Introduction and factors influencing the seasonal

429   growth of trees. Springer, New York.

430   44. George SS, Meko DM, Evans MN (2008) Regional tree growth and inferred summer climate in

431   the Winnipeg River basin, Canada, since AD 1783. Quaternary Res 70: 158-172.

432   45. Shi J, Liu Y,Vaganov E et al (2008) Statistical and process-based modeling analyses of tree

433   growth response to climate in semi-arid area of north central China: A case study of *Pinus*

434   *tabulaeformis*. J. Geophys Res-Biogeo 113: G01026**.**

435   46. Zhang YX, Shao XM, Xu Y, Wilmking M (2011) Process-based modeling analyses of *Sabina*

436   *przewalskii* growth response to climate factors around the northeastern Qaidam Basin. Sci Bull

437   56: 1518-1525.

438   47. Gou X, Zhou F, Zhang Y et al (2013) Forward modeling analysis of regional scale tree-ring

439   patterns around the northeastern Tibetan Plateau, Northwest China. Biogeo Discuss 2013:

440   9969-9988.

441   48. Oribe Y, Funada R, Shibagaki M et al (2001) Cambial reactivation in locally heated stems of the

442   evergreen conifer *Abies sachalinensis* (Schmidt) Masters. Planta 212: 684-691.

443   49. Gričar J, Zupančič M, Čufar K et al (2006) Effect of local heating and cooling on cambial activity

444   and cell differentiation in the stem of Norway spruce (*Picea abies*). Ann Bot 97: 943-951.

445   50.Huang JG, Deslauriers A, Rossi S (2014) Xylem formation can be modeled statistically as a

446   function of primary growth and cambium activity. New Phytol 203: 831-841.

447   51. Wang ZY, Yang B, Deslauriers A et al (2015) Intra-annual stem radial increment response of

448   Qilian juniper to temperature and precipitation along an altitudinal gradient in northwestern

449   China. Trees - Struct Funct 29:25-34.

450   52. Lupi C, Morin H, Deslauriers A et al (2012) Xylogenesis in black spruce: does soil temperature

451   matter? Tree Physiol 32: 74-82.

452   53. Hosoo Y, Yoshida M, Imai T et al (2002) Diurnal difference in the amount of

453   immunogold-labeled glucomannans detected with field emission scanning electron microscopy at

454   the innermost surface of developing secondary walls of differentiating conifer tracheids. Planta

455   215: 1006-1012.

456   54. Steppe K, Sterck F, Deslauriers A (2015) Diel growth dynamics in tree stems: linking anatomy

457   and ecophysiology. Trends Plant Sci 20: 335-343.

458   55. Dünisch O (2010) Low night temperatures cause reduced tracheid expansion in *Podocarpus*

459   *latifolius*. IAWA J 31: 245-255. https://doi.org/10.1163/22941932-90000020

460   56. Boulouf Lugo J, Deslauriers A, Rossi S (2012) Duration of xylogenesis in black spruce

461   lengthened between 1950 and 2010. Ann Bot 110: 1099-1108.

462   57. Körner C (2015) Paradigm shift in plant growth control. Curr Opin Plant Biol 25: 107-114.

463 58. Li M, Xiao W, Wang S et al (2008) Mobile carbohydrates in Himalayan treeline trees I. Evidence

464 for carbon gain limitation but not for growth limitation. Tree Physiol 28: 1287-1296.

465 59. Wiley E, Helliker B (2012) A re-evaluation of carbon storage in trees lends greater

466 support for carbon limitation to growth. New Phytol 195: 285-289.

467

468

469

470

471

472

473

474

475

476

477

478

479

480

481

482

483

484

485

486   **Table 1** Mean (±standard deviation) of the threshold daily maximum (MaxT), mean (MeanT)

487   and minimum (MinT) temperatures for the onset and ending of xylogenesis.

488

		Onset of xylogenesis			Ending of xylogenesis		
Site	Year	MinT(°C)	MeanT(°C)	MaxT(°C)	MinT(°C)	MeanT(°C)	MaxT(°C)
1	2007	0.6±0.2	4.3±0.1	9.7±0.4	0.8±0.3	3.9±0.3	9.0±0.4
	2008	0.8±0.2	3.7±0.3	8.9±0.4	0.6±0.2	3.5±0.2	8.7±0.1
	2009	0.8±0.3	4.4±0.1	9.8±0.2	1.1±0.1	4.7±0.1	9.9±0.1
	2010	0.3±0.1	3.4±0.2	9.1±0.3	0.4±0.1	2.9±0.3	8.0±0.2
2	2007	0.5±0.3	4.3±0.2	9.4±0.5	0.9±0.4	4.1±0.5	9.3±0.6
	2008	1.0±0.3	3.9±0.3	8.7±0.4	0.7±0.3	3.6±0.2	8.7±0.1
	2009	0.8±0.3	4.4±0.4	9.8±0.2	1.1±0.3	4.5±0.4	9.8±0.3

489

490

491

492

493

494

495

496

497

498

499

500

501

502 **Table 2** Mean (±standard deviation) of degree-day sums (≥5°C) at onset of xylogenesis,

503 number of days from the date of snow melting (Date$_{snow}$) and soil thawing (Date$_{soil}$) to the

504 onset date of xylogenesis (Date $_{xylogenesis}$).

	Year	Degree-day sum at onset of xylogenesis (DD)	Number of days between Date$_{snow}$ and Date $_{xylem}$ (days)	Number of days between Date$_{soil}$ and Date $_{xylem}$ (days)
Site 1	2007	41±13	4±5	4±3
	2008	11±0	18±3	6±3
	2009	8±2	29±3	11±3
	2010	8±3	46±3	29±5
Site 2	2007	34±20	6±5	6 ±3
	2008	13±12	21±4	9 ±5
	2009	12±7	29±3	11±3

505

506

507

508

509

510

511

512

513

514

515

516

517   **Table 3** The best-fit parameter estimates for the VS model used in this study.

Model parameter	Description(unit)	Value
CT_{min}	Minimum temperature for tree growth (°C)	0.9
T_{opt1}	Lower end of range of optimal temperatures (°C)	5.9
T_{opt2}	Upper end of range of optimal temperatures	9.3
T_{max}	Maximum temperature for tree growth (°C)	19.9
W_{min}	Minimum soil moisture for tree growth (v/v)	0.06
W_{opt1}	Lower end of range of optimal soil moisture (v/v)	0.18
W_{opt2}	Upper end of range of optimal soil moisture (v/v)	0.22
W_{max}	Maximum soil moisture for tree growth (v/v)	0.50
T_{beg}	Temperature sum for initiation of growth (°C)	30
D_{root}	Depth of root system (mm)	50
P_{max}	Maximum daily precipitation for saturated soil (mm)	20
K_1	Fraction of precipitation penetrating soil (dimensionless)	0.86
K_2	First coefficient for calculation of transpiration (mm/day)	0.12
K_3	Second coefficient for calculation of transpiration (1/ °C)	0.175
K_r	Coefficient for water infiltration from soil (dimensionless)	0.006

518

519

Figure captions:

521 **Fig. 1** Micrometeorological conditions (2007 - 2010) at the upper treeline in the Sygera Mts.,

522 southeastern Tibetan Plateau, showing (a) daily mean air temperature and daily total

523 precipitation, (b) daily soil temperature (at depths of 10, 20 and 40 cm) and snow depth, and

524 (c) daily mean soil volumetric moisture contents (at depths of 10, 20 and 40 cm).

525

526 **Fig. 2** Onset (a), ending (b), and duration (c) of xylem formation of Smith fir (*Abies georgei*

527 var. *smithii)* based on weekly xylogenesis observations at site 1 (4360 m a.s.l.) (grey columns)

528 and site 2 (4250 m a.s.l.) (white columns). Error bars indicate standard deviations among

529 trees.

530

531 **Fig. 3** Lagged (0–10 days) Pearson correlation coefficients between xylem cell production (a,

532 b), growth index (c, d), and corresponding climatic variables. P0 represents the weekly

533 climatic mean for the exact period between two sampling dates. P1 to P10 represent the

534 weekly means lagged 1–10 days before the sampling date. Dotted horizontal lines show the

535 95% confidence limits. *Abbreviations*: MaxT = maximum temperature, MeanT= mean

536 temperature, MinT= minimum temperature, P = precipitation, and GGD = growing degree

537 days above 5°C.

538

539 **Fig. 4** Critical minimum (black dots), mean (white dots), and maximum (grey dots) air

540 temperatures at sites 1 and 2, corresponding with the 0.5-probability of the onset and ending

541   of xylem formation according to xylogenesis observations in Smith fir. Error bars indicate the

542   standard deviation among trees.

543

544   **Fig. 5** Observed (solid line) and simulated (dashed line) tree-ring width indices at Smith fir

545   treeline in the Sygera Mts. on the southeastern Tibetan Plateau, 1960–2006.

546

547   **Fig. 6** Pearson correlation coefficients between the observed and estimated values of tree-ring
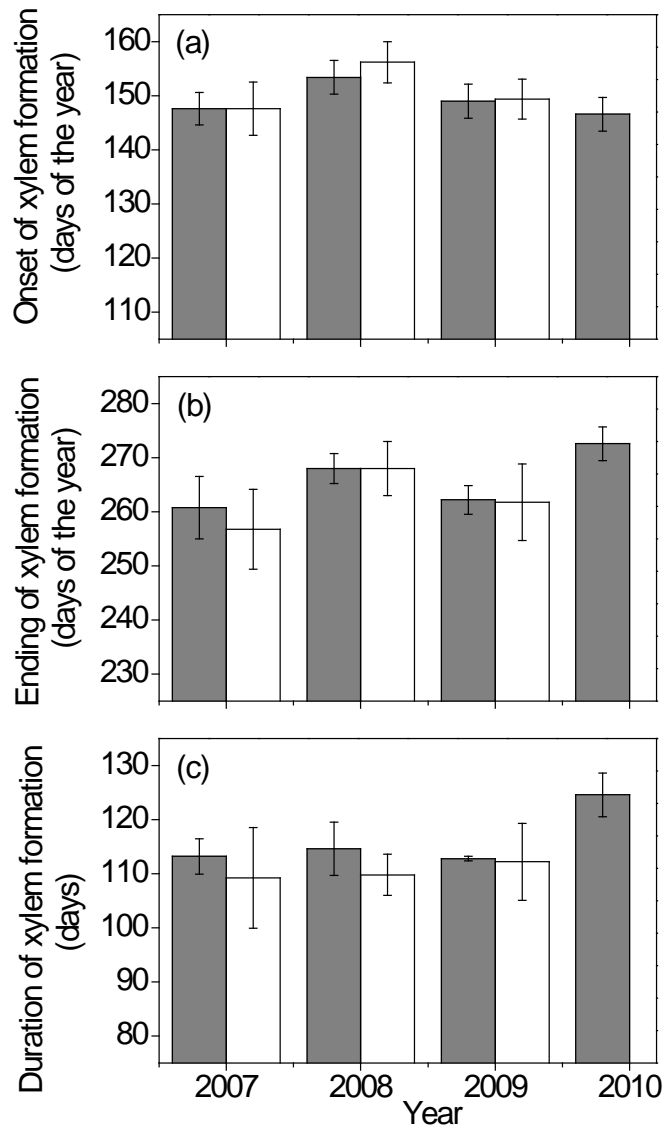
548   width for different estimates of CT_{min}.

549

550
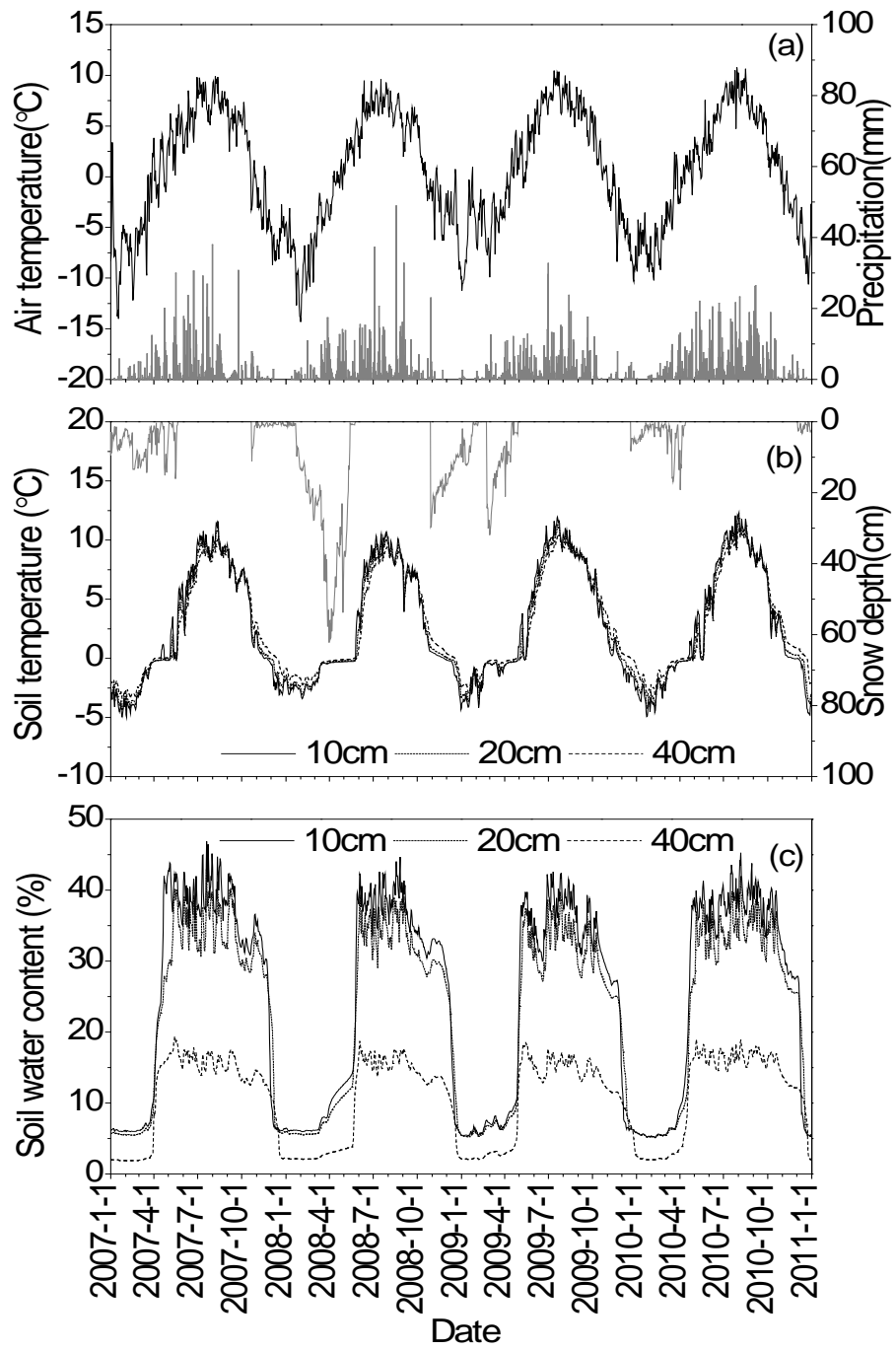
551

552　　　　Fig. 1

553

554

555   Fig. 2

556

557

558

559

560

561

562

563

Fig. 3

566

25
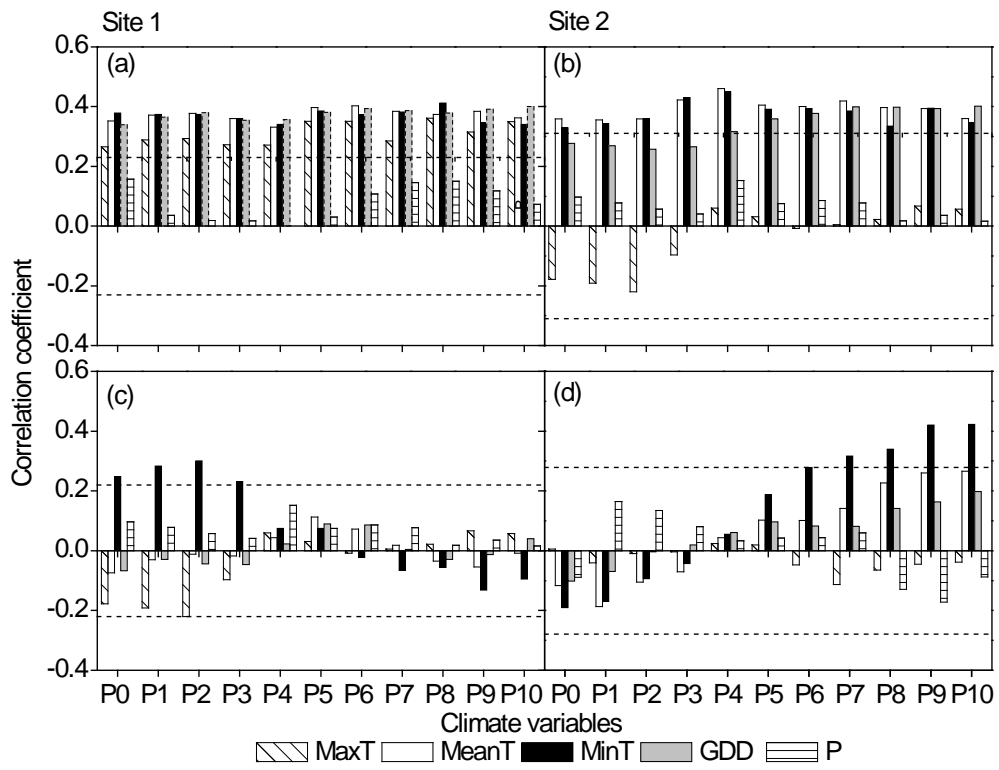
577
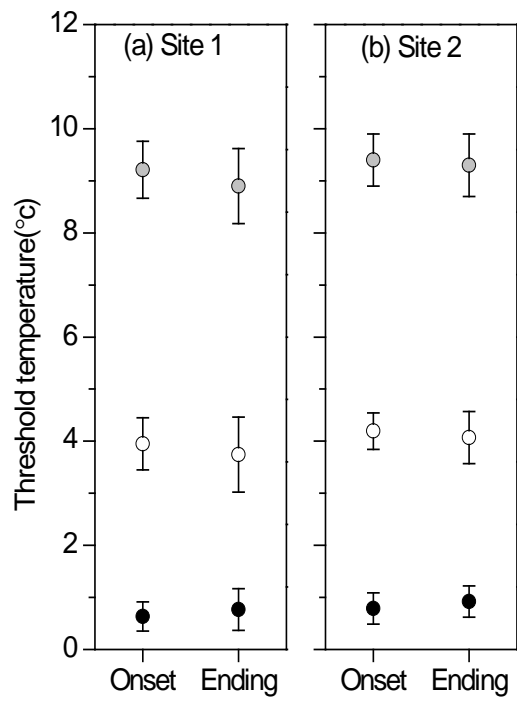
578

579   Fig. 4

580

581

582

583

584
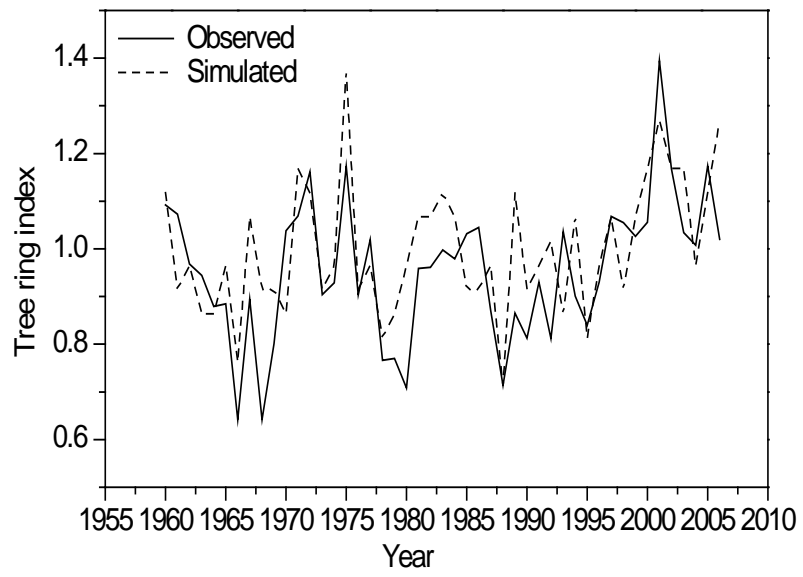
585

586

587

588

589

590

591

592

593   Fig. 5

594
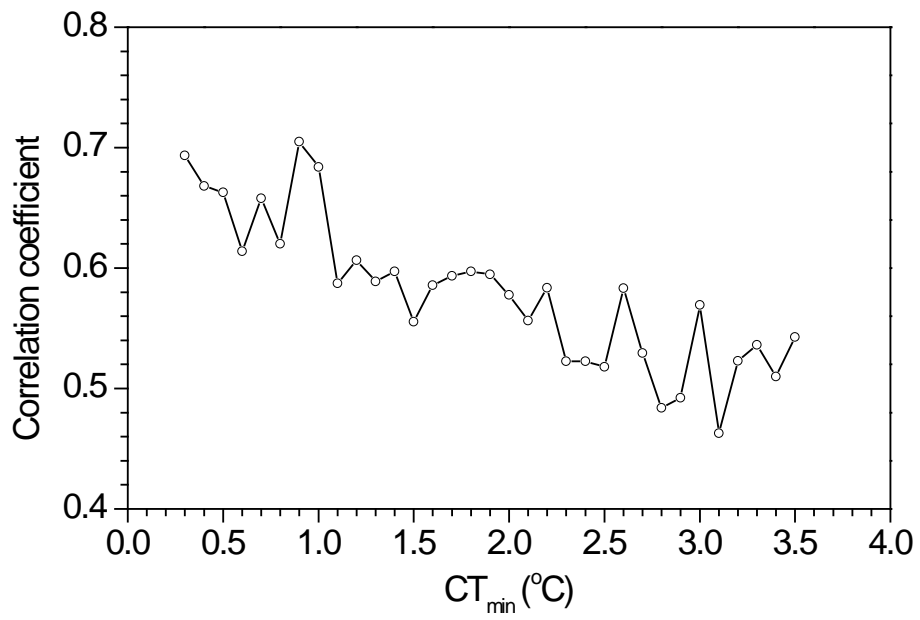
595

596

597

598

599

600

601

602

603

604

605

606

607

608

609

610   Fig. 6

611

612

1   **Supplementary content**

2   **Table S1** Parameters of the Gompertz function (A, ß, K), R^2 and day of the inflection

3   point (tp) for Smith fir growing at two treeline sites, 2007 – 2010.

	Year	A	ß	K(10^{-2})	tp	R^2
Site 1	2007	23.95	5.48	3.25	170.59	0.98
	2008	22.97	5.97	3.32	179.32	0.96
	2009	25.68	7.07	4.08	174.50	0.96
	2010	21.08	5.67	3.25	176.67	0.99
Site 2	2007	24.79	5.03	2.85	176.56	0.98
	2008	21.22	6.97	3.87	178.13	0.98
	2009	23.62	5.70	3.02	188.53	0.98

4

5

6

7
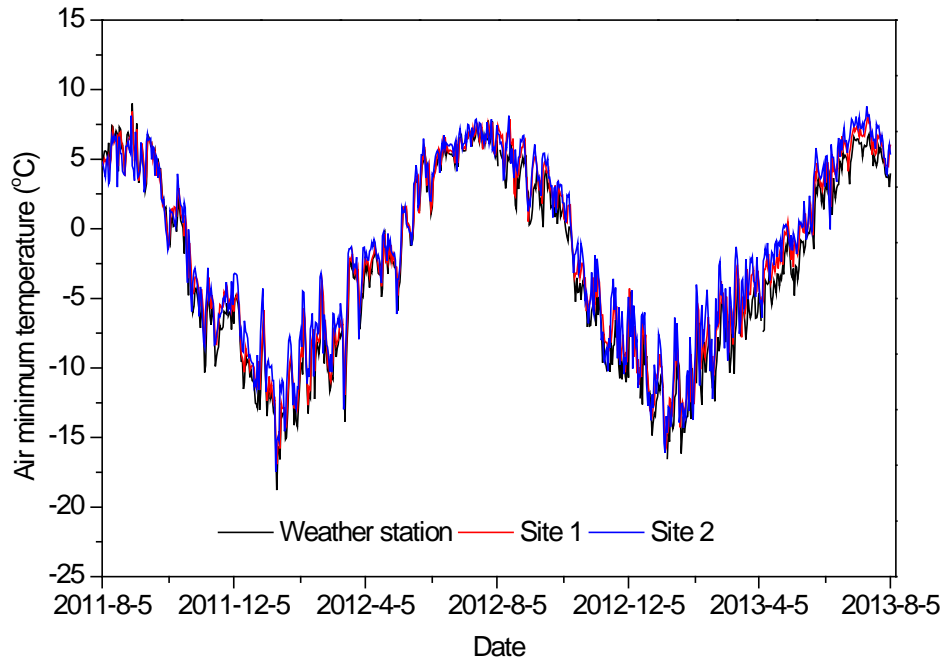
8

9

10

11

12

13

14
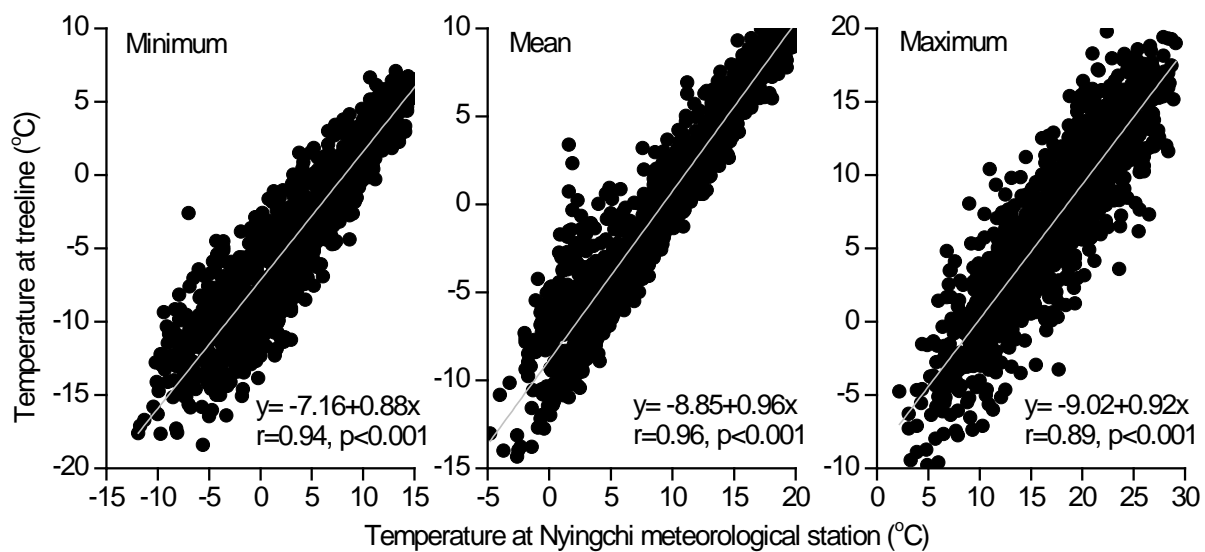
15

16   **Fig. S1.** Plots of the daily minimum, mean, and maximum temperature from automatic

17   weather stations at treeline in the Sygera Mountains and at the Nyingchi meteorological

18   station from January 1, 2007 to December 31, 2010.

19

20

21

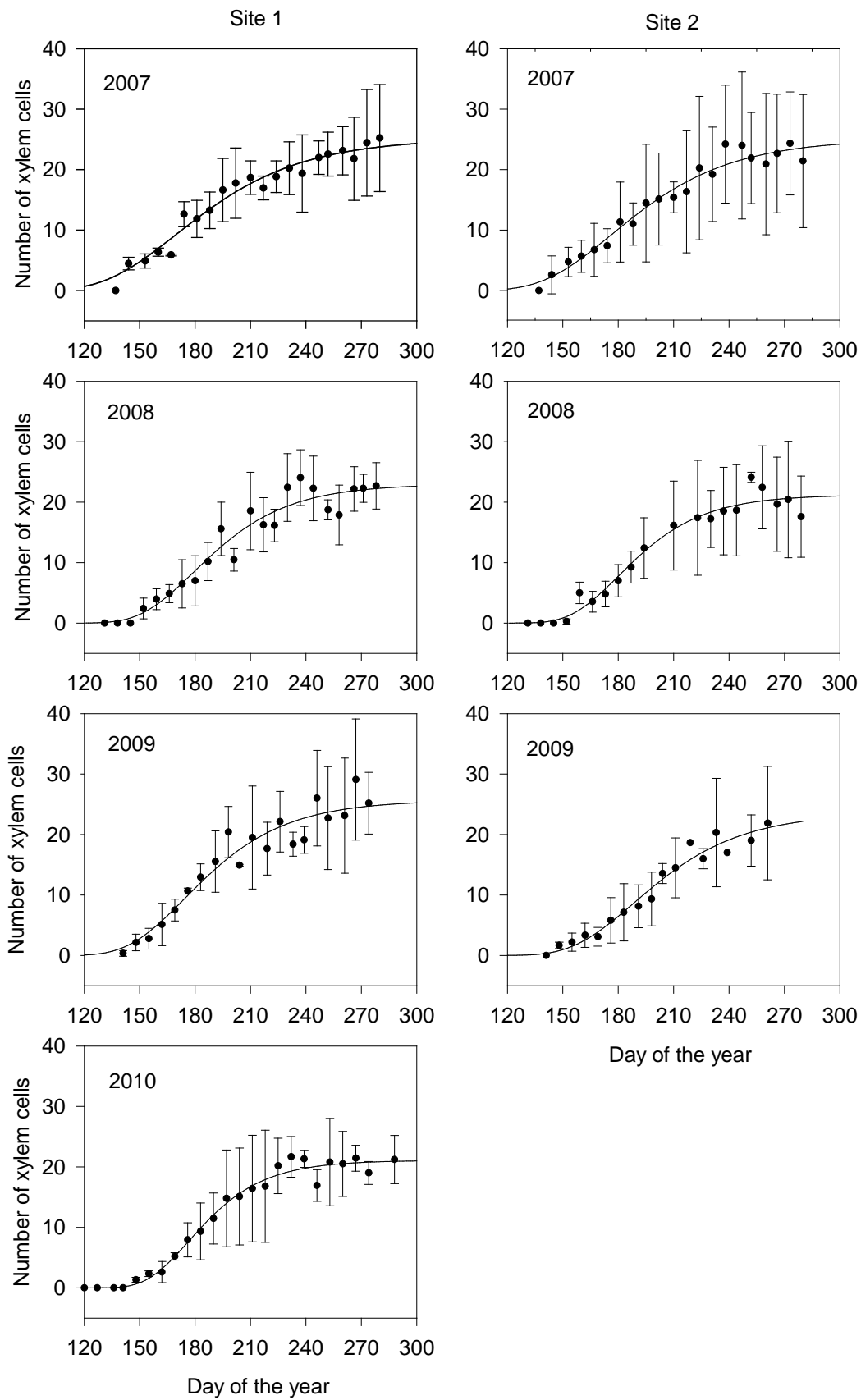**Fig. S2.** Minimum air temperatures recorded by the automatic weather station (black line)

and temperature data logger (TidbiT v2 Temp UTBI-001, Onset Computer Corporation,

Bourne, MA, USA) at site 1 (red line) and site 2 (blue line) from August 5, 2011 to August 5,
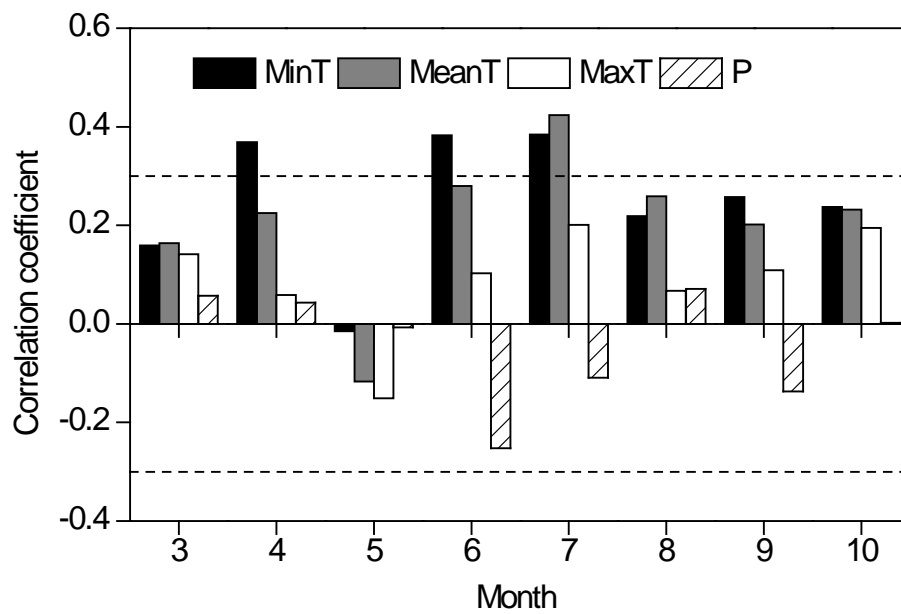
2013.

26

27

Fig. S3. Dynamics of xylem growth (including enlarging, wall thickening, and mature xylem

29   cells) at two Smith fir treelines as modeled using a Gompertz function.

30

31
32

33 **Fig. S4**. Correlations between the simulated tree ring chronology and monthly temperature

34 and precipitation at Smith fir treeline in the Sygera Mountains on the southeastern Tibetan

35 Plateau. Dotted horizontal lines show the 95% confidence limits. *Abbreviations*: MaxT =

36 maximum temperature, MeanT= mean temperature, MinT= minimum temperature and P =

37 precipitation.

38
39